Remote Sensing of Environment 204 (2018) 448–455

Contents lists available at ScienceDirect

Remote Sensing of Environment

journal homepage: www.elsevier.com/locate/rse

Modeling grassland above-ground biomass based on artificial neural network and remote sensing in the Three-River Headwaters Region

Shuxia Yang[a,b], Qisheng Feng[a,b], Tiangang Liang[a,b,*], Baokang Liu[c], Wenjuan Zhang[a,d], Hongjie Xie[e]

[a] State Key Laboratory of Grassland Agro-ecosystems, College of Pastoral Agriculture Science and Technology, Lanzhou University, Lanzhou 730020, China
[b] Key Laboratory of Grassland Livestock Industry Innovation, Ministry of Agriculture, China
[c] Qinghai Institute of Meteorological Sciences, Xining 810001, China
[d] Qinghai Province Grassland Stations, Xining 810001, China
[e] Laboratory for Remote Sensing and Geoinformatics, Department of Geological Sciences, University of Texas at San Antonio, TX 78249, USA

ARTICLE INFO

Keywords:
Alpine grassland
MODIS
Accuracy assessment
Mean impact value

ABSTRACT

Effective and accurate monitoring of grassland above-ground biomass (AGB) is important for pastoral agriculture planning and management. In this study, we combined 1433 AGB field measurements and remotely sensed data with the goal of establishing a suitable model for estimating grassland AGB in the Three-River Headwaters Region (TRHR) of China, which is one of the most sensitive regions to the warming climate. A back-propagation artificial neural network (BP ANN) was used to select the variables that contribute the most to the model's estimation of AGB, and then we built the model. Out of 13 variables, 5 variables were selected to build the BP ANN model, and we used cross validation for the accuracy assessment. The results show that: (1) the modeled mean AGB (2001–2016) provides a reasonable spatial distribution that is similar to the field measurements but reveals more details and has better spatial coverage than the limited field measurements are able to provide; (2) the overall trend of AGB in the TRHR is increasing more than decreasing (44.4% vs 29.2%, respectively) and has a stable area of 26.4%; and (3) the BP ANN model achieves better results than do the traditional multi-factor regression models (R^2: 0.75–0.85 vs 0.40–0.64, RMSE: 355–462 vs 537–689 kg DW/ha). This study presents an effective and operational BP ANN model that estimates grassland AGB for the study area with high accuracy at 500 m spatial resolution, providing a scientific basis for the determination of reasonable stocking capacity and possible future development.

1. Introduction

Grassland is an important component of terrestrial ecosystem that plays a vital role in protecting the ecological environment and preventing erosion (Wang et al., 2009; Liu et al., 2011). Grassland is the material foundation for the development of the national economy in pastoral areas, and it functions as a natural barrier that provides land eco-environmental protection. The Three-River headwaters region (TRHR) is important for its large area of grassland and wetland ecosystem (Zhang et al., 2012; Li et al., 2013b; Tong et al., 2014). As China's most extensive wetland, the TRHR has abundant river, lake, mountain snow, and glacier resources and is known as one of the world's largest alpine wetland ecosystem. Due to its special geographical location, rich natural resources, and distinguished ecological function, the TRHR is an important nature reserve in the Qinghai-Tibet Plateau, China (Liu et al., 2008b; Liu et al., 2014; Zhang et al., 2012; Tong et al., 2014). However, the region's high altitude and harsh natural conditions make its ecosystem extremely fragile. In recent years, the ecosystem has undergone large changes from climate warming and increasing human activities (Jiang and Zhang, 2016). Estimating the grassland biomass timely and accurately and establishing suitable forecasting model can provide a scientific basis for determining a reasonable stocking capacity (Yang et al., 2012). Grassland above-ground biomass (AGB) monitoring methods are categorized into two groups: ground-based and remote sensing methods. The ground-based methods traditionally involve cutting the grass in the field, drying it, and weighing it in the laboratory. However, this approach is time consuming and costly; consequently, it is applicable only for small-scale monitoring (Xu et al., 2008). With the advances in space-borne sensor technology and increase in spatial and temporal resolutions, satellite remote sensing is now regarded as the best choice for large-scale monitoring (Claverie et al., 2012). The remote sensing-based methods

* Corresponding author.
E-mail address: tgliang@lzu.edu.cn (T. Liang).

http://dx.doi.org/10.1016/j.rse.2017.10.011
Received 29 March 2017; Received in revised form 27 September 2017; Accepted 9 October 2017
Available online 19 October 2017
0034-4257/

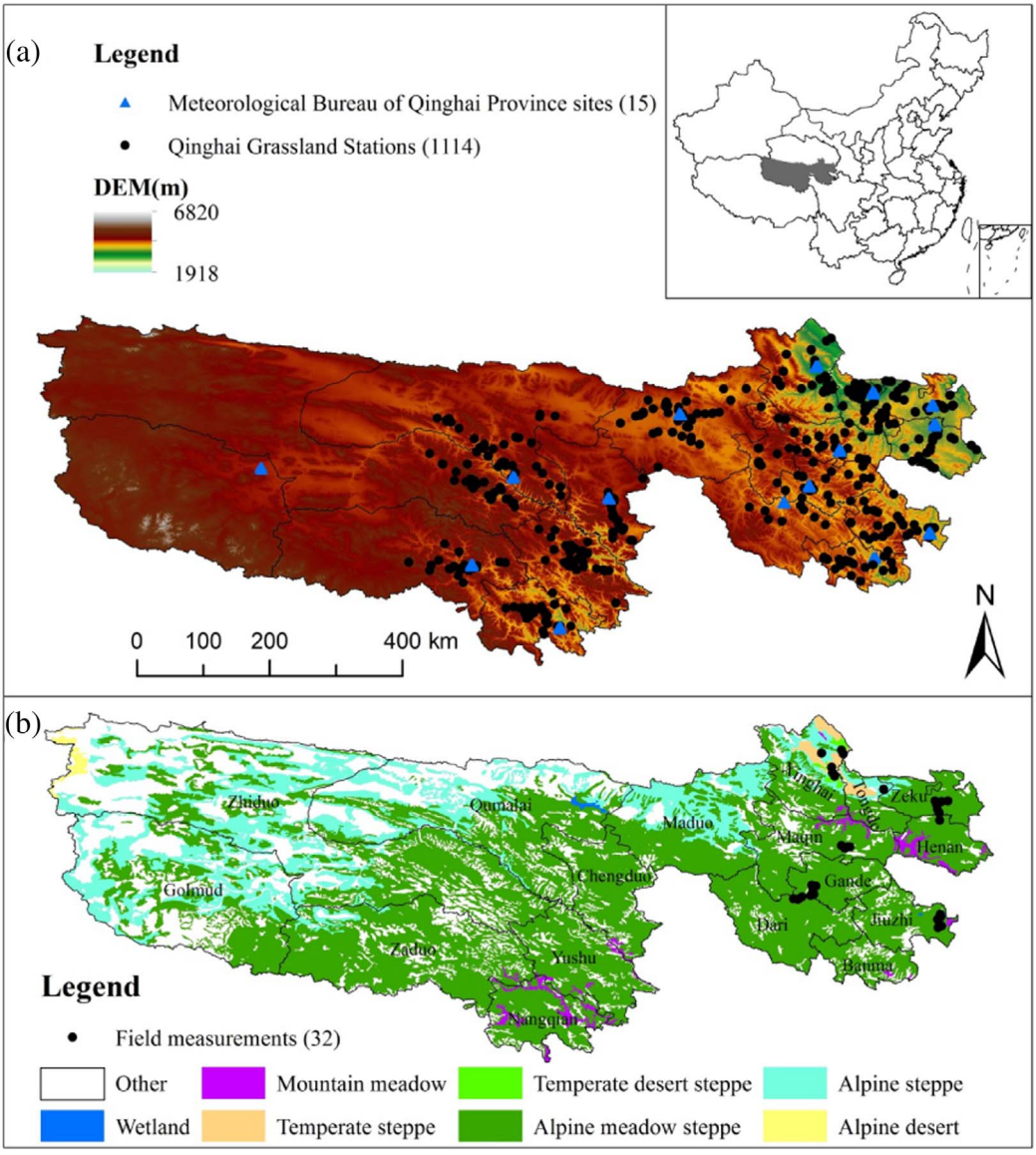

Fig. 1. Observation sites from three different sources: (a) Meteorological Bureau of Qinghai Province sites (15 sites with 287 effective AGB data) and Qinghai Grassland Stations (1114 effective AGB data) overlaid on an elevation map; and (b) the 32 effective AGB field measurement sites of this study in the Three-River Headwaters Region, China. The background elevation data used in (a) are from the Shuttle Radar Topography Mission.

for grassland biomass estimation can be grouped into regression (statistical) and machine learning algorithm models (Ali et al., 2016).

The remotely sensed normalized difference vegetation index (NDVI) has been used to study the health and biomass of natural grasslands since the 1970s (Ullah et al., 2012; Li et al., 2014; Zhao et al., 2014). In addition to the NDVI, other vegetation indexes (VIs) have been used, including but not limited to the soil-adjusted vegetation index (SAVI) (Huete et al., 1985; Huete, 1988), the modified soil-adjusted vegetation index (MSAVI) (Qi et al., 1994), the enhanced vegetation index (EVI) (Garroutte et al., 2016), and the narrow-band vegetation index (Jacques et al., 2014). Studies have indicated that the MSAVI can reduce the influence of soil background, and it is particularly useful for estimating the AGB of sparsely vegetated grassland areas (Gilabert et al., 2002). The EVI can enhance the sensitivity to high vegetation areas, where NDVI saturation occurs at a leaf area index over 2.0–2.5 (Baret and Guyot, 1991; Huete et al., 2002). However, most of the previous studies involved statistical models based on a single VI, and each has its own limitations and uncertainties (Zhao et al., 2014).

The Artificial Neural Network (ANN) model belongs to a powerful class of empirical modeling algorithms that are capable of computing, predicting and classifying data and are more versatile than regression models (Ali et al., 2016). The Back Propagation (BP) ANN has been used to estimate forest biomass (Wang and Guan, 2007; Liu et al., 2008a; Wang and Xing, 2008; Wang et al., 2017) and crop yields, e.g., corn and rice (Panda et al., 2010). However, only limited studies have focused on grassland biomass estimation. Xie et al. (2009) compared the performances of ANN and regression models for AGB estimation in the Xilingol River Basin, Inner Mongolia, by using topographic, vegetation index and spectral information from Landsat ETM + as inputs. The ANN accuracy was R^2 = 0.82 and its RMSEr was 40.61%, which were better than those of the regression model (R^2 = 0.60 and RMSEr = 50.08%). Yang et al. (2012) used the ANN algorithm for grassland biomass estimation based on five vegetation indices derived from MODIS and found that the ANN models were more accurate (R^2 = 0.56–0.71) than the statistical models (R^2 = 0.54–0.68). Vahedi (2016) developed both site-specific allometric equations and ANN models for predicting tree biomass and found that the best ANN model, using the Tan-sig function, resulted in lower error (R^2 = 0.91, RMSE% = 7.37), compared with the allometric equations (R^2 = 0.88, RMSE% = 8.83). Li et al. (2013a) used single and multi-temporal remotely sensed data to estimate grassland biomass with both statistical and ANN models and found that the use of multi-temporal remotely sensed data has advantages for AGB estimation and that the ANN achieved higher accuracy for AGB estimation. Although studies have shown that it is difficult to determine

instructive rules via the *black box* operation of ANN models, such models can obtain relatively high accuracy, and ANN models can be used to estimate grassland AGB at large scales (Wang and Guan, 2007). Therefore, exploring and establishing a high-accuracy grassland AGB model based on the BP ANN approach has become an important research topic that has important practical significance for improving the current grassland AGB monitoring methods based on remote sensing data.

A recent study on the TRHR (Liang et al., 2016) presented a multi-factor non-linear regression model based on geographic location (x, y) and grass cover and height. This model greatly improved the accuracy of AGB estimation and reduced the RMSE by 222.1 kg DW/ha compared with the single MODIS NDVI-based AGB model. However, this model was based on field measurements from only 15 stations, and the modeled results did not reflect a realistic distribution of AGB estimation in the area. Based on lessons learned from Liang et al.'s (2016) paper, this study proposes a completely new approach, based on a massive (over 1433 samples) set of long-term field measurements and the BP-ANN algorithm. Its major objectives are (1) to develop a multi-factor-based ANN model; and (2) to analyze the temporal and spatial changes of the grassland AGB of the TRHR from 2001 to 2016, under the warming climate conditions.

2. Methodology

2.1. Study area and observation sites

The TRHR (E 100°53′ ~ 102°16′, N 34°05′ ~ 34°55′) is located in the hinterland of the Qinghai-Tibet Plateau (Fig. 1a), and it is the headwater source of the three largest rivers in China: the Yellow River, the Yangtze River and the Lancang River. This area belongs to the 3 autonomous prefectures in the TRHR, including 14 counties whose primary industry is animal husbandry. The total grassland area is 20,989,700 ha, while the area of usable grassland is 17,874,400 ha. The area has an average elevation of over 4000 m and an average annual temperature of − 5.6 to 4.9 °C. Its annual precipitation is 615.5 mm and occurs mostly from June to September. Because summer is short, the grass growth period is also short, resulting in low-growing plants and low yields. The cold season extends for 7–8 months. The major types of grassland include alpine meadow steppe and alpine steppe, which account for approximately 76% and 23% of the total grassland, respectively (Fig. 1b).

The grass observation data stem from three different sources: (1) the Meteorological Bureau of Qinghai Province, including 15 meteorology and grassland monitoring sites with a total of 287 effective AGB measurements for the period of 2003 to 2014; the specific observation time is during the last one to two days of July and August of each year (Liang et al., 2016) (Fig. 1a); (2) Qinghai Grassland Stations, including a once-monthly data collection (from the end of June to October) during the growing season (June to October) comprising 1114 effective AGB measurements from 2010 to 2014 (Yang et al., 2016) (Fig. 1a); and (3) field measurements from this study, including 32 effective AGB measurements from August (at the end of August) of 2015 (Fig. 1b). In this study, data source (2) is used to develop the models and data sources (1) and (3) are used for model evaluation.

The sampling methods of the above three data sources were identical: each grassland observation site consists of a 3–5 km × 1–2 km rectangular area with a dominant grass type; each site includes 3–5 sampling quadrants in two different sizes: 0.5 m × 0.5 m for relatively homogeneous grass and 1.0 m × 1.0 m for complex and inhomogeneous grass. Data source (1) consists of fixed observations; data sources (2) & (3) contain randomly sampled data. However, all the observation sites were all-natural grassland with no human interaction during the study period. The data recorded from each quadrant included latitude, longitude, elevation, aspect, slope, grass type, coverage, height, fresh weight, and dry weight (oven-dried at 65 °C for 48 h in the lab). All the AGB values (from dry weights) in one MODIS pixel (500 m × 500 m) were averaged to represent the mean AGB for the MODIS pixel, and the center latitude and longitude of the pixel were used for modeling purposes.

2.2. Elevation data

The Digital Elevation Model (DEM) data consists of 90 m Shuttle Radar Topography Mission (SRTM) images (version 004) (http://srtm.csi.cgiar.org) in Geo-Tiff format. To match the available data, the digital elevation data was resampled to 500 m, and the projection type was defined as Albers map projection. For further analysis, ArcGIS software was used to extract the longitude, latitude and elevation of the pixels corresponding to the ground samples.

2.3. MODIS data and processing

The MODIS surface reflectance product (MOD09GA) was obtained from NASA'S Earth Observing System Data and Information System (EOSDIS) (https://earthdata.nasa.gov/). The data include daily surface reflectance of MODIS bands 1–7 at 500 m resolution. Two scenes were required to cover the entire area in a day. Therefore, a total of 4846 scenes were downloaded for the 2423 days (25 days had no available data) during the grassland growth period (from June to October) over the 16-year period (2001–2016).

The data preprocessing included the following steps: (1) the MODIS Reprojection Tool (MRT) was employed to transform and register daily MOD09GA reflectance data to Albers map projection (Geo-Tiff format). (2) The daily reflectance data were processed using ArcGIS software (ESRI, Redlands, CA, USA) to obtain daily values of the VIs (NDVI, EVI and RVI) (Table 1). The 5 band indices (B7/B2, B2–B7, B7/B5, B5/B7, and (B5–B7)/(B5 + B7) (Jacques et al., 2014) (flagged bad values and cloud pixels were not included in the processing and calculations). (3) To minimize the cloud effects (no values were available when covered by clouds), the daily images of VIs and band indices were processed to produce the monthly maximum composites of VIs and band indices for the study area in each year of 2001 to 2016 for further analysis.

2.4. Grassland coverage inversion

The field-measured grassland coverage from the data source (2) and the corresponding (collocated and concurrent) monthly MODIS EVI values derived from the MOD09GA product as detailed in Section 2.3 were paired and used to develop an inversion model for grassland coverage as shown in Fig. 2. The grassland coverage data derived from this equation ($y = 45.421\ln(x) + 101.95$, R^2 is 0.53, here x is the MODIS EVI) were used to develop grassland biomass inversion models and to derive the time series grassland biomass from 2001 to 2016 used

Table 1
Indicator screening for the ANN AGB models.

Variables	MIV	Accumulative contribution
Coverage (C)	0.2224	52.37%
NDVI (N)	0.0814	71.53%
Height (H)	0.0333	79.37%
Latitude (Y)	0.0207	84.26%
Longitude (X)	0.0197	88.91%
RVI	0.0154	92.54%
EVI	0.0094	94.76%
B7/B2	0.0080	96.64%
B7/B5	0.0056	97.94%
B5/B7	0.0044	98.98%
(B5–B7)/(B5 + B7)	0.0025	99.57%
DEM(m)	0.0018	99.99%
B2–B7	0.0000	100.00%

C: grass cover, X: longitude, Y: latitude, H: grass height, and N: NDVI.

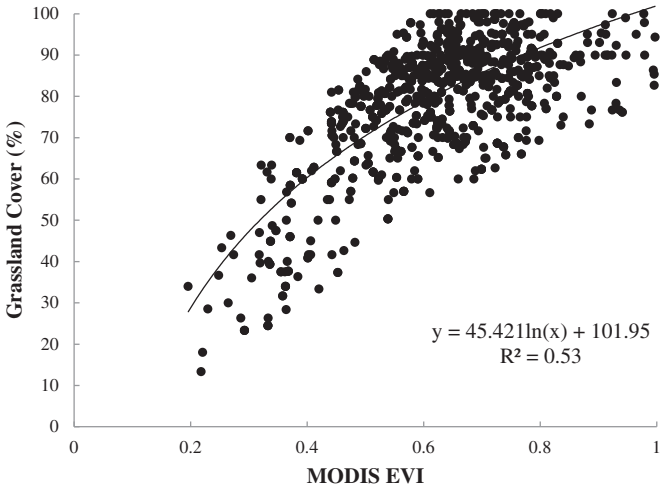

Fig. 2. The grassland coverage inversion model based on MODIS EVI in the Three-River Headwaters Region (data source 2 with n = 1114).

later in the paper.

2.5. BP ANN model construction and cross validation

There has been a substantial increasing interest in using ANN for biomass estimation during the last 15 years (Kumar et al., 2015). ANN, one of the most commonly modeling techniques, has a highly interconnected structure similar to human brains that emulates the operations and connectivity of biological neurons (Özçelik et al., 2010; Tiryaki and Aydın, 2014). The BP neural network refers to a multi-layer network structure that consists of an input layer, an output layer and one or more hidden layers. Some studies have reported that BP neural networks can efficiently handle non-linear relationships among data even when there are conflicting relationships between the explanatory variables and the dependent variables (Moghadassi et al., 2010). A number of methods are available to examine ANN inputs and to select only the significant independent variables by excluding the less significant independent variables. In this study, we consider 13 variables: topography (DEM), vegetation biophysical indicators (grassland height and coverage), geographical location (latitude and longitude), and the remote sensing vegetation indices (NDVI, EVI, RVI, B7/B2, B2–B7, B7/B5, B5/B7), and (B5–B7)/(B5 + B7). The variables used to establish biomass model were chosen when they had accumulative Mean Impact Values (MIV) of at least 85% (Fu et al., 2012; Shi et al., 2012; Gu and Xie, 2013; Jiang et al., 2013; Wu et al., 2016; Wang et al., 2017).

To design the network for optimal topology, the optimal numbers of hidden layers and neurons were determined based on a trial-and-error process (Tiryaki and Aydın, 2014). All the input data were normalized within the boundary (0–1) for modeling in ANN (Naghdi and Ghajar, 2012) and the input consisted of a training set, test set, and validation set. The training set was used to adjust the weights on the neural network. The test set was used only for testing the final solution to confirm the true predictive power of the network. The test set has no effect on training; it provides an independent measure of network performance during and after training. The validation set was used to minimize overfitting. Training automatically stops when generalization stops improving, as indicated by the stop decreasing or even increasing mean squared error (MSE) between the measured values and model outputs in the validation samples (Ali et al., 2016). In this study, the Levenberg-Marquardt function algorithm was selected for ANN training. By combining different hidden layers and training functions, we constructed a grassland AGB model based on the BP ANN.

We evaluated the performance of our model based on a 10-fold cross validation method (Jung et al., 2011; Liu et al., 2017). For the current study, using 10 folds resulted in the shortest validation test time with acceptable bias and variance. Therefore, 10-fold cross validation was used to ensure effective generalization (Chou and Pham, 2017). The data source (2) was split into 10 approximately equal numbers of samples (i.e., 10 parts) used for the 10-fold cross validation. Each time, a different part (i.e., 1/10 of total samples) was used as test set and a different part as the validation set; the remaining 8 parts were used as the training set. R^2 and RMSE values were calculated for each dataset (Huang and Gao, 2017). This process was repeated 10 times until each of the 10 parts had been employed as both a test set and as part of the training set. The R^2 and RMSE values from the 10 runs were averaged to obtain the final R^2 and RMSE values of the model's performance. To compare the linear and non-linear models with the ANN models, the same 10-fold cross validation method and the same data source (2), 1114 AGB field measurements were applied. For each run, a different part (i.e., 1/10 of total samples) was used as the test set and the remaining 9 parts were used as the training set. The R^2 and RMSE values of the 10 runs were then averaged to obtain the final R^2 and RMSE values of the model's performance. The BP ANN model and its validation were implemented using the MATLAB Neural Network toolbox.

2.6. Trend analysis

The grassland AGB change trend was analyzed by using the slope over the period from 2001 to 2016. The slope model uses a linear trend analysis (Stow et al., 2003); the inter-annual change ratio of grassland AGB in TRHR is calculated on a pixel-by pixel-basis (500 m × 500 m) from 2001 to 2016, so that the growth situation of grassland vegetation can be examined spatially. The formula for the slope is

$$\text{Slope} = \frac{n \times \sum_{i=1}^{n} i \times \text{Biomass}_i - \sum_{i=1}^{n} i \sum_{i=1}^{n} \text{Biomass}_i}{n \times \sum_{i=1}^{n} i^2 - \left(\sum_{i=1}^{n} i\right)^2},$$

where Biomass_i is the growing season maximum grassland aboveground biomass of the i-th year, and n is the cumulative monitored years (16). In this study, i covers the years from 2001 to 2016.

For further discussion of the spatial distribution pattern of grassland growth, the slope was categorized into significantly decreasing (< − 20 kg DW/ha yr), decreasing (− 20–− 10 kg DW/ha yr), stable (− 10–10 kg DW/ha yr), increasing (10–20 kg DW/ha yr) and significantly increasing (> 20 kg DW/ha yr) (Dong et al., 2011; Zhao et al., 2015).

3. Results

3.1. Spatial distribution of AGB from all field measurements of 2003–2015

The generalized spatial distribution of AGB measurements during 2003–2015 provides an overall picture of the AGB values of the study area (Fig. 3). As shown in the figure, the AGB values range between 30 and 4380 kg DW/ha (mean 1086.42 ± 776.76 kg DW/ha). Because there were no AGB measurements (only one station) in the far western part of the study area, the discussion here focuses on the eastern portion of the study area. The overall trend of AGB values decreases from the southeast to the northwest (of the eastern portion of the study area), with some exceptions. For example, some very low AGB values (< 400 kg DW/ha) can be seen in the very southeast corner in Jiuzhi and Banma counties, while the highest AGB values (> 1600 kg DW/ha) are in Zeku, Henan, Tongde and Maqin counties. The most wide-spread low AGB values (< 800 kg DW/ha) occur in the north-central counties: Zhiduo, Qumalai, Chengduo, and Maduo (for all county names, please refer to Fig. 1).

3.2. Accuracy assessment of the ANN model

Table 1 lists the degree ranking of 13 variables with their MIV

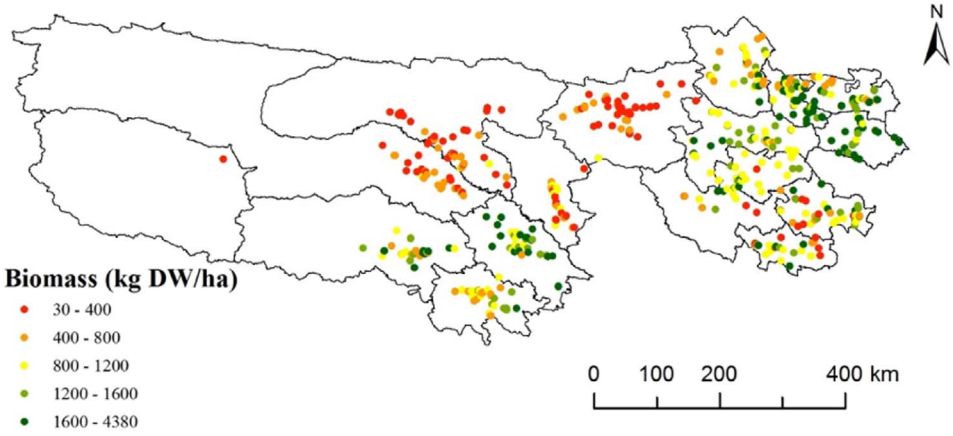

Fig. 3. Measured maximum above-ground biomass (AGB) for the period of 2003–2015 (n = 1161), including 1114 sites from the Qinghai Grassland Station, 32 sites from this study, and 15 sites of the meteorological stations (all AGB values measured at each meteorological station are averaged for that station).

Table 2
Accuracy assessment of the ANN models using 10-fold cross validation method.

Variable composites	Training set		Validation set		Test set	
	R^2	RMSE	R^2	RMSE	R^2	RMSE
CXYHN	0.85	355.04	0.68	537.09	0.66	556.57
CXYH	0.84	362.56	0.68	533.09	0.66	561.64
CXYN	0.80	410.32	0.62	589.86	0.59	611.49
CXHN	0.80	410.65	0.63	577.63	0.62	593.96
CXY	0.79	421.88	0.65	570.22	0.65	559.25
CHN	0.75	462.77	0.57	619.78	0.60	591.80

values. Five variables: grass coverage (C), longitude (X), latitude (Y), height (H), and the NDVI (N) accounted for 88.91% of the cumulative MIV contribution and are subsequently further used. The 10-fold cross validation results (R^2 and RMSE values) of the ANN AGB models (CXYHN, CXYH, CXYN, CXHN, CXY, and CHN) are shown in Table 2, including the results on the three different datasets: the training, test, and validation sets. Clearly, the six models' performances are best on the training set (higher R^2 and lower RMSE), followed by the validation set and then the test set. The models based on the training dataset reflect 75–85% of the variations in the grassland AGB. The CXYHN model performed best, followed by the CXYH model. However, these two models include the grass height variable, which is currently impossible to directly measure from the satellite-based remote sensing with sufficient spatial and temporal resolution; and grass height modeled from other parameters could inherit large uncertainties and errors (Liang et al., 2016). Considering that the CXYN model, including geographical location, vegetation coverage and index, has a higher R^2 and a lower RMSE on the training set compared with the CXY model, the CXYN model is selected for this study (see Section 3.4) to produce the AGB maps from 2001 to 2016 used for spatial and temporal analyses.

3.3. Comparison between ANN models and multi-factor regression models

To further confirm that the ANN models perform better than other regression models in estimating AGB for the study area, the same 1114 samples and 10-fold cross validation method are used here to construct multi-factor linear and non-linear regression models based on the same six variable composites using the same five variables (Table 1) selected by the ANN MIV method. As shown in Table 3, the non-linear models are better than the corresponding linear models (0.46–0.64 vs. 0.40–0.58 for R^2, 537–657 vs. 576–689 kg DW/ha for RMSE on the training dataset). These values are considerably worse compared with those of the ANN models (0.75–0.85 for R^2 and 355–462 kg DW/ha for RMSE on the training dataset, Table 2). This result clearly confirms that the ANN model developed in this study performs better than do the multi-factor regression models.

Table 3
Accuracy assessment of the multiple regression models using the 10-fold cross validation method.

Variable composites	models	Training set		Test set	
		R^2	RMSE	R^2	RMSE
CXYHN	linear	0.58	576.50	0.57	578.95
	non-linear	0.64	537.70	0.63	540.99
CXYH	linear	0.56	592.06	0.55	594.59
	non-linear	0.59	573.88	0.58	577.39
CXYN	linear	0.43	670.41	0.43	671.73
	nonlinear	0.55	603.37	0.54	607.06
CXHN	linear	0.58	576.61	0.57	578.46
	non-linear	0.63	539.61	0.62	542.35
CXY	linear	0.40	689.54	0.40	690.57
	non-linear	0.46	657.68	0.45	660.15
CHN	linear	0.58	579.31	0.57	580.64
	non-linear	0.63	542.18	0.62	544.35

C: grass cover, X: longitude, Y: latitude, H: grass height, and N: NDVI.

3.4. Spatial distribution of grassland AGB based on the ANN

As discussed above, the ANN model based on grass cover, longitude, latitude and the NDVI (i.e., the CXYN model) was selected to simulate the average AGB for yearly grassland in the TRHR for the 16 study years. To evaluate the accuracy of the grassland biomass inversion based on the CXYN model established from data source(2), we compared the estimated results with the measured values from the data sources (1) and (3) (Fig. 4). The results show that the CXYN model reflects 76% of the variation in the grassland AGB, obtaining an RMSE of 594.53 kg DW/ha.

Fig. 5 shows that the overall spatial distribution of grassland AGB from 2001 to 2016 has a pattern similar to that obtained from the field measurements (Fig. 3), but includes many more details that are impossible to obtain from the limited field measurements even with > 13 years of effort. For example, in the far west of the study area, Fig. 5 clearly shows a low AGB distribution, which is reasonable, considering the higher elevation and overall cold climate there. The overall high AGB in the far east also matches well with Fig. 3. The far eastern area is the primary pastoral agricultural area of the TRHR. The central area of the TRHR (Maduo, Qumalai, Zaduo, northwestern Chengduo, and easternmost Zhiduo counties) has an overall moderate AGB of approximately 2000 kg DW/ha.

In the past 16 years, overall, the grassland AGB showed more of an increasing than a decreasing trend (44.4% vs. 29.2%, respectively), and have a stable area of 26.4% (Fig. 6). The far eastern (Zeku and Henan) and the far southwestern (portions of Golmud and Yushu) regions of the study area had the most significant increasing (16.5%), while the far northwestern portion of Zhiduo had the most significant decreasing

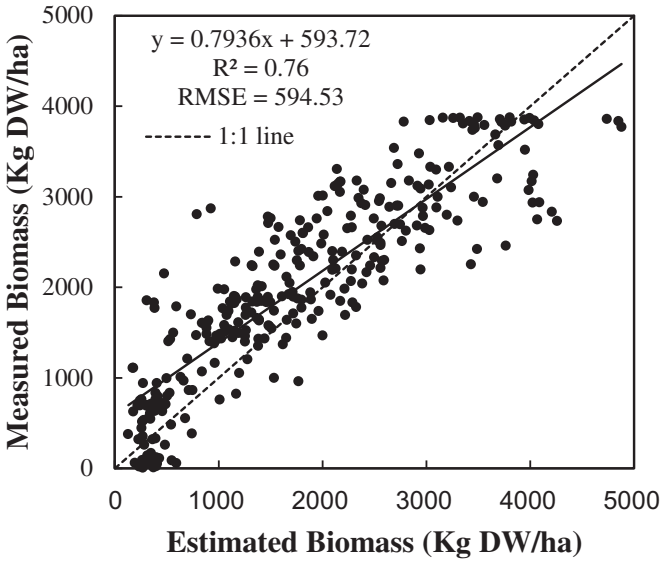

Fig. 4. The relationship between the estimated biomass based on the CXYN model and the measured biomass.

(3.8%). AGB decreased but not significantly in 25.4% of the study area, and most of these lie in the triangle areas of Maduo, Chengduo, and Qumalai. AGB increased but not significantly in 27.9% of the study area, primarily distributed in the south (Zaduo and Nangqian), outside of the two significantly increasing areas.

4. Discussion

4.1. Advantages and disadvantages of using artificial neural networks in grassland AGB estimations

Using an ANN to estimate grassland AGB has the following advantages. First, this model can estimate any complex non-linear relationship. Second, all the quantitative and qualitative information is distributed within the network of neurons, which are robust and fault tolerant. Third, rapid and massive operations are possible by applying parallel processing. In practice, ANN models have been shown to be superior to other traditional methods in terms of data accuracy, processing speed, and non-linear problem solving (Ali et al., 2016; Deo and Sahin, 2017); therefore, the BP neural network has been widely applied to leaf area indexes based on hyperspectral grassland AGB estimations or inversions.

However, problems can occur when estimating grassland AGB. Compared with the traditional statistical models, an ANN has obvious limitations; for example, the accuracy of the learning process depends on the quantity and quality of the samples, and the convergence process can be slow or suffer from local minima problems. In addition, the underlying mechanisms of parallel information processing and distributed storage for ANN models are not well understood. Moreover, the theoretical basis for selecting a reasonable network structure is insufficient. As a *black box* method, the geometry of an ANN presents a complicated architecture. Although the best network may provide good results for a specific set of data, it may not provide accurate results for another set of data. This situation is usually caused by the over-fitting problem of an ANN model. The optimal numbers of hidden layers and nodes depend on the problem itself and the repeated tests. When the number of nodes in the hidden layer is too small, the algorithm will not be able to focus on the reverse propagation to reach the minimum value during training. In contrast, when the number of nodes in the hidden layer is too large, the network will suffer from over-fitting. The over-fitting problem cannot be ignored when applying an ANN.

The ANN model solves the corresponding problem related to the weight of network convergence; but it does not guarantee that the solution is optimal; therefore, repeated training is required to obtain an optimal neural network and achieve reasonable results. Although the neural network solves multi-factor linear and non-linear problems and obtains higher accuracy than the traditional statistical models, the neural network training processes and the model equations cannot be observed; therefore, it is sometimes difficult to explain the ANN results from a theoretical perspective.

4.2. Factors affecting the accuracy of remote sensing grassland AGB estimation models

Although it achieves higher accuracy and lower estimation error, the BP ANN model can still suffer from inheritance problems. First, spatial-temporal inconsistencies can occur between the sampling sites and the satellite data (Eisfelder et al., 2012). Temporal disparities between the monthly maximum value of the MODIS VIs and the field-measured biophysical parameters during the peak period of grass growth are unavoidable, even with the best efforts. In terms of spatial consistency, the sampling sites are relatively small, whereas each pixel in the MODIS data covers a 500 m × 500 m area. In this study, to test other band indices, we used the daily reflectance data of the 500 m resolution images to produce the monthly maximum composites of VIs, and used the band indices to remove the bad pixels and cloud pixels. However, in future, based on the results from this study, the MODIS monthly EVI and NDVI 500 m resolution products should be able to be used directly for ANN modeling.

Second, areas with complicated topography, slope and topographical factors have a certain impact on the vegetation reflectance, which might have impacted the MODIS retrieval of NDVI and EVI and,

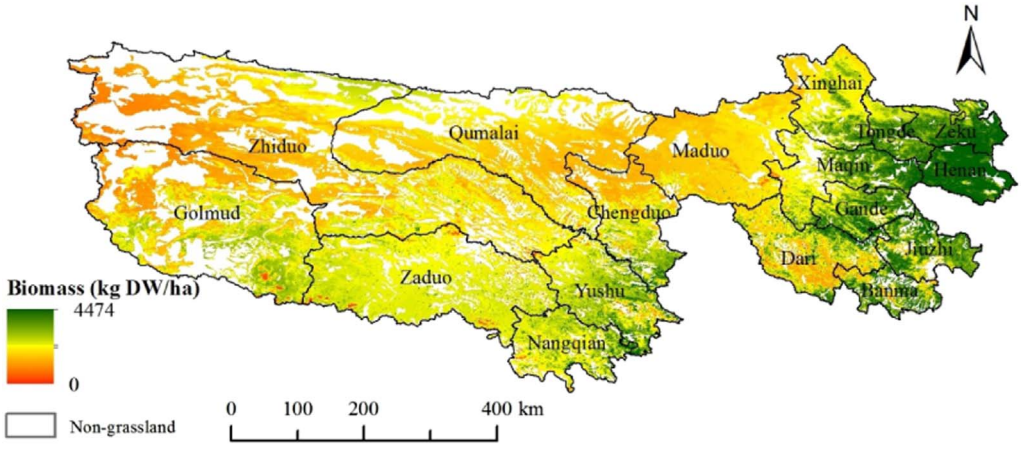

Fig. 5. Spatial distribution of the average grassland AGB in the TRHR from 2001 to 2016.

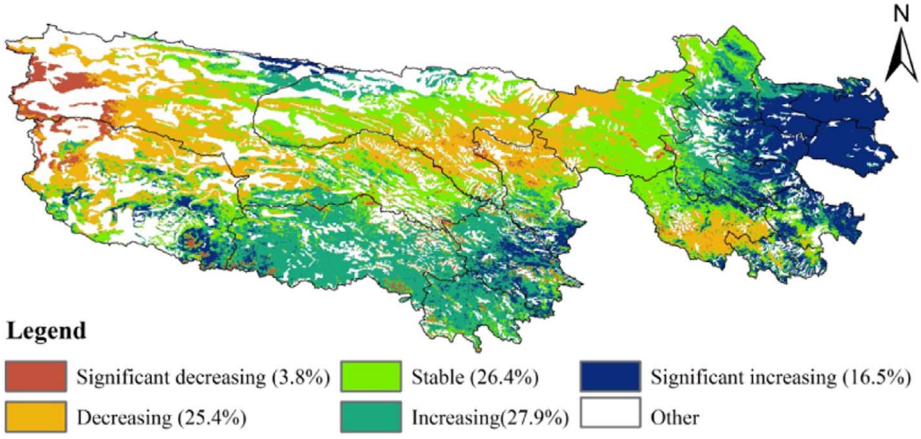

Fig. 6. Change trend of grassland AGB in the TRHR from 2001 to 2016.

subsequently, the derivation of the grass cover variable. Grassland tends to degrade when it is sparse. These degraded and/or naked spots could affect the remotely sensed reflectivity, which would affect the NDVI and EVI and, eventually, affect the building of the ANN model.

Third, uncertainties in the measured data could also introduce errors during model development. On one hand, the different locations and harvest targets employed in these studies may have contributed to such differences. Generally, we lay out sample plots in relatively homogenous areas, including field experimental plans and field investigations. Thus, the sample plots will produce errors for some heterogeneous areas (Jia et al., 2016). On the other hand, the representativeness of a sample plot is highly important when calibrating model parameters and performing validation. However, due to the influences derived from the heterogeneity of the land surface, the positioning accuracy of GPS, topography, and even traffic conditions, there are always matching and/or representativeness problems when matching the sample plots to the corresponding pixels. These are also common problems in quantitative remote sensing. In this study, each grassland observation site is a 3–5 km × 1–2 km rectangular area with a dominant grass type; each site includes 3–5 sampling quadrants in two different sizes: 0.5 m × 0.5 m for relatively homogeneous grass and 1.0 m × 1.0 m for complex and inhomogeneous grass, while each MODIS pixel represents a square of 500 m, which is much larger than the sample plots sizes. This disparity inevitably produces some modeling errors (Yuan et al., 2016).

In addition, the measured data of grassland biomass are mainly distributed among the middle and eastern areas of the TRHR; samples from the western area are rare due to data source restrictions and high altitudes. This could also introduce some degree of uncertainties to the model—especially for the western part of the study area. Finally, to some extent, the accuracy of the grass cover inversion model based on the EVI could also affect the AGB inversion accuracy.

5. Conclusions

This study collected 1433 measurements of above-ground biomass (AGB) from the Three-River Headwaters Region (TRHR) from 2003 to 2015. This massive field-based data provides an overall picture of the AGB distribution in the study area. The highest AGB can clearly be seen in the easternmost and central-north portion of the study area, primarily in Zeku, Henan, Tongde and Maqin counties. This massive field-based data also functioned as the basis for variable selection, the development of the BP ANN models for AGB estimation, and for the evaluation of the model's accuracy. Out of 13 possible variables, 5 variables were selected using the ANN Mean Impact Value (MIV) method, and these 5 variables were subsequently used to build the model and for comparison purposes. The 5 variables selected are grass coverage (C), longitude (X), latitude (Y), height (H) and the NDVI (N). Although the best BP ANN model is the one based on a combination of all five variables, the model based only on CXYN was selected as the final model for AGB estimation from 2001 to 2016 due to its easy operational aspect. The modeled mean AGB (2001–2016) showed a reasonable spatial distribution that was similar to the distribution of the field measurements but with many more details and far more spatial coverage than the limited field measurements (although over 1000 samples) were able to provide. We found that the overall trend of AGB in the TRHR is increasing more than decreasing (44.4% vs. 29.2%, respectively), with a stable area of 26.4%. The far eastern (Zeku and Henan) and the far southwestern (portions of Golmud and Yushu) regions of the study area experienced significant AGB increasing (16.5%), while the far northwestern portion of Zhiduo experienced a significant decreasing (3.8%). Although the neural network model achieves higher accuracy than do the traditional statistical models, the training process and the equations of the ANN model cannot be observed; therefore, the internal mechanisms of this model cannot be easily explained. In future work, we plan to compare the advantages and disadvantages of different machine learning algorithms (ANN, Support Vector Machine and Random Forest) to establish the best grassland biomass inversion model. Another approach to improvement would be to find a better inversion model for grassland coverage estimation, because grassland coverage plays a key role in improving grassland biomass monitoring. It is our intention to use unmanned aerial vehicles (UAVs) to obtain better and more accurate mapping of grassland vegetation coverage. Thereby, a better grass cover inversion model based on the MODIS EVI could be constructed and, eventually, the accuracy of grassland biomass monitoring from remote sensing and modeling would improve.

Acknowledgments

This study was supported by the Program for Changjiang Scholars and Innovative Research Team in University (IRT_17R50), the National Natural Science Foundation of China (31672484, 31372367, 31702175, 41101337 and 41401472), the Consulting Project of Engineering Academy of China (2016-XZ-38) and the Fundamental Research Funds for the Central Universities (lzujbky-2017-k01). Authors would like to thank the three anonymous reviewers for their very helpful comments, suggestions, and corrections that substantially improved the paper.

References

Ali, I., Cawkwell, F., Dwyer, E., Barrett, B., Green, S., 2016. Satellite remote sensing of grasslands: from observation to management—a review. J. Plant Ecol. 9 (6), 649–671.

Baret, F., Guyot, G., 1991. Potentials and limitations of vegetation indices for LAI and APAR assessment. Remote Sens. Environ. 3, 161–173.

Chou, J.S., Pham, A.D., 2017. Nature-inspired metaheuristic optimization in least squares support vector regression for obtaining bridge scour information. Inf. Sci. 399, 64–80.

Claverie, M., Demarez, V., Duchemin, B., 2012. Maize and sunflower biomass estimation

in southwest France using high spatial and temporal resolution remote sensing data. Remote Sens. Environ. 124 (6), 844–857.
Deo, R.C., Sahin, M., 2017. Forecasting long-term global solar radiation with an ANN algorithm coupled with satellite-derived (MODIS) land surface temperature (LST) for regional locations in Queensland. Renew. Sust. Energ. Rev. 72, 828–848.
Dong, J.W., Tao, F.L., Zhang, G.L., 2011. Trends and variation in vegetation greenness related to geographic controls in middle and eastern Inner Mongolia, China. Environ. Earth Sci. 62, 245–256.
Eisfelder, C., Kuenzer, C., Dech, S., 2012. Derivation of biomass information for semi-arid areas using remote-sensing data. Int. J. Remote Sens. 33 (9), 2937–2984.
Fu, Z.G., Qi, M.F., Jing, Y., 2012. In: Regression forecast of main steam flow based on mean impact value and support vector regression. Proceedings of the 2012 IEEE Conference on Power and Energy Engineering, Kota Kinabalu, Malaysia, 2–5 December 2012.
Garroutte, E.L., Hansen, A.J., Lawrence, R.L., 2016. Using NDVI and EVI to map spatiotemporal variation in the biomass and quality of forage for migratory elk in the Greater Yellowstone ecosystem. Remote Sens. 8 (5), 404.
Gilabert, M.A., González-Piqueras, J., GarcíA-Haro, F.J., 2002. A generalized soil-adjusted vegetation index. Remote Sens. Environ. 82 (2), 303–310.
Gu, Y., Xie, H., 2013. In: Research on the secondary generation of virtual human body based on customer shape in 3D fitting system. The 8th International Conference on Computer Science & Education (ICCSE 2013) April 26–28, 2013. Colombo, Sri Lanka. pp. 757–760.
Huang, J.C., Gao, J.F., 2017. An ensemble simulation approach for artificial neural network: an example from chlorophyll a simulation in Lake Poyang, China. Eco. Inform. 37, 52–58.
Huete, A.R., 1988. A soil-adjusted vegetation index (SAVI). Remote Sens. Environ. 25 (3), 195–213.
Huete, A.R., Jackson, R.D., Post, D.F., 1985. Spectral response of a plant canopy with difference soil backgrounds. Remote Sens. Environ. 17 (1), 37–53.
Huete, A.R., Didan, K., Miura, T., Rodriguez, E.P., Gao, X., Ferreira, L.G., 2002. Overview of the radiometric and biophysical performance of the MODIS vegetation indices. Remote Sens. Environ. 83 (1–2), 195–213.
Jacques, D.C., Kergoat, L., Hiernaux, P., Mougin, E., Defourny, P., 2014. Monitoring dry vegetation masses in semi-arid areas with MODIS SWIR bands. Remote Sens. Environ. 153, 40–49.
Jia, W.X., Liu, M., Yang, Y.H., He, H.L., Zhu, X.D., Yang, F., Yin, C., Xiang, W.N., 2016. Ecol. Indic. 60, 1031–1040.
Jiang, C., Zhang, L., 2016. Ecosystem change assessment in the Three-river Headwater Region, China: patterns, causes, and implications. Ecol. Eng. 93, 24–36.
Jiang, J.L., Su, X., Ding, H.T., Zhou, P.P., Han, S.N., Yuan, Y.J., 2013. A novel approach to evaluate the quality and identify the active compounds of the essential oil from l. Anal. Lett. 46 (46), 1213–1228.
Jung, M., Reichstein, M., Margolis, H.A., Cescatti, A., Richardson, A.D., Arain, M.A., Arneth, A., Bernhofer, C., Bonal, D., Chen, J., Gianelle, D., Gobron, N., Kiely, G., Kutsch, W., Lasslop, G., Law, B.E., Lindroth, A., Merbold, L., Montagnani, L., Moors, E.J., Papale, D., Sottocornola, M., Vaccari, F., Williams, C., 2011. Global patterns of land–atmosphere fluxes of carbon dioxide, latent heat, and sensible heat derived from eddy covariance, satellite, and meteorological observations. J. Geophys. Res. Biogeo. 116 (G3), 245–255.
Kumar, R., Aggarwal, R.K., Sharma, J.D., 2015. Comparison of regression and artificial neural network models for estimation of global solar radiations. Renew. Sust. Energ. Rev. 52, 1294–1299.
Li, W.H., Zhao, X.Q., Zhang, X.Z., Shi, P.L., Wang, X.D., Zhao, L., 2013a. Change mechanism in main ecosystems and its effect of carbon source/sink function on the Qinghai-Tibetan Plateau. Chinese. J. Nature 35, 172–178.
Li, F., Jiang, L., Wang, X.F., Zhang, X.Q., Zheng, J.J., Zhao, Q.J., 2013b. Estimating grassland aboveground biomass using multitemporal MODIS data in the West Songnen Plain, China. J. Appl. Remote. Sens. 7 (1), 73546-1-16.
Li, F., Zeng, Y., Li, X.S., Zhao, Q.J., Wu, B.F., 2014. Remote sensing based monitoring of interannual variations in vegetation activity in China from 1982 to 2009. Sci. China Earth Sci. 57 (8), 1800–1806.
Liang, T.G., Yang, S.X., Feng, Q.S., Liu, B.K., Zhang, R.P., Huang, X.D., Xie, H.J., 2016. Multi-factor modeling of above-ground biomass in alpine grassland: a case study in the three-river headwaters region, china. Remote Sens. Environ. 186 (1), 164–172.
Liu, J.Y., Xu, X.L., Shao, Q.Q., 2008a. The spatial and temporal characteristics of grassland degradation in the three-river headwaters region in Qinghai Province. Acta Geograph. Sin. 63 (4), 364–376.
Liu, Z., Chang, Y., Chen, H., 2008b. Estimation of forest volume in Huzhong forest area based on RS, GIS and ANN. Chin. J. Appl. Ecol. 19 (9), 1891–1896 (In Chinese).
Liu, X.Y., Long, R.J., Shang, Z.H., 2011. Evaluation method of ecological services function and their value for grassland ecosystems. Acta Pratacult. Sin. 20 (1), 167–174 (In Chinese).
Liu, X.F., Zhang, J.S., Zhu, X.F., Pan, Y.Z., Liu, Y.Z., Zhang, D.H., Lin, Z.H., 2014. Spatiotemporal changes in vegetation coverage and its driving factors in the Three-River Headwaters Region during 2000–2011. J. Geogr. Sci. 24 (2), 288–302.
Liu, Y., Bi, J.W., Fan, Z.P., 2017. Multi-class sentiment classification: the experimental comparisons of feature selection and machine learning algorithms. Expert Syst. Appl. 80 (2017), 323–339.
Moghadassi, A.R., Nikkholgh, M.R., Parvizian, F., 2010. Estimation of thermosphysical properties of dimethyl ether as a commercial refrigerant based on artificial neural networks. Expert Syst. Appl. 37 (12), 7755–7761.
Naghdi, R., Ghajar, I., 2012. Application of artificial neural network in the modeling of skidding time prediction. Adv. Mater. Res. 403-408, 3538–3543.
Özçelik, R., Diamantopoulou, M.J., Brooks, J.R., 2010. Estimating tree bole volume using artificial neural network models for four species in Turkey. J. Environ. Manag. 91 (3), 742–753.
Panda, S.S., Ames, D.P., Panigrahi, S., 2010. Application of vegetation indices for agricultural crop yield prediction using neural network techniques. Remote Sens. 2, 673–696.
Qi, J., Chehbouni, A., Huete, A.R., Kerr, Y.H., Sorooshian, S., 1994. A modified soil adjusted vegetation index. Remote Sens. Environ. 48 (2), 119–126.
Shi, H., Lu, Y., Du, J., Du, W., Ye, X., Yu, X., 2012. Application of back propagation artificial neural network on genetic variants in adiponectin adipoq, peroxisome proliferator-activated receptor-γ, and retinoid x receptor-α genes and type 2 diabetes risk in a Chinese Han population. Diabetes Technol. Ther. 14 (3), 293–300.
Stow, D., Daeschner, S., Hope, A., Douglas, D., Petersen, A., Myneni, R., Zhou, L., Oechel, W., 2003. Variability of the seasonally integrated normalized difference vegetation index across the north slope of Alaska in the 1990s. Int. J. Remote Sens. 24, 1111–1117.
Tiryaki, S., Aydın, A., 2014. An artificial neural network model for predicting compression strength of heat treated woods and comparison with a multiple linear regression model. Constr. Build. Mater. 62, 102–108.
Tong, L., Xu, X., Fu, Y., 2014. Wetland changes and their responses to climate change in the three-river headwaters region of China since the 1990. Energies 7, 2515–2534.
Ullah, S., Si, Y.L., Schlerf, M., Skidmore, A.K., Shafique, M., Iqbal, I.A., 2012. Estimation of grassland biomass and nitrogen using MERIS data. Int. J. Appl. Earth Obs. Geoinf. 19 (1), 196–204.
Vahedi, A.A., 2016. Artificial neural network application in comparison with modeling allometric equations for predicting above-ground biomass in the Hyrcanian mixed-beech forests of Iran. Biomass Bioenergy 88, 66–76.
Wang, S., Guan, D., 2007. Remote sensing method of forest biomass estimation by artificial neural network models. Ecol. Environ. 16 (1), 108–111 (In Chinese).
Wang, L., Xing, Y., 2008. Remote sensing estimation of natural forest biomass based on an artificial neural network. Chin. J. Appl. Ecol. 19 (2), 261–266 (In Chinese).
Wang, X.X., Zhu, J.Z., Fan, Y.M., 2009. Research on dynamics estimation models of grassland based on MODIS-NDVI in the middle section of northern hillside Tianshan Mountain. Pratacult. Sci. 26 (7), 24–27.
Wang, L., Liu, J.P., Xu, S.H., Dong, J.J., Yang, Y., 2017. Forest above ground biomass estimation from remotely sensed imagery in the mount tai area using the RBF ANN algorithm. Intell. Autom. Soft Comput. http://dx.doi.org/10.1080/10798587.2017.1296660.
Wu, Z.Y., Lei, X.J., Zhu, D.W., Luo, A.M., 2016. Investigating the variation of volatile compound composition in maotai-flavoured liquor during its multiple fermentation steps using statistical methods. Food Technol. Biotechnol. 54 (2), 243–249.
Xie, Y., Sha, Z., Yu, M., Bai, Y., Zhang, L., 2009. A comparison of two models with Landsat data for estimating above ground grassland biomass in Inner Mongolia, China. Ecol. Model. 220, 1810–1818.
Xu, B., Yang, X.C., Tao, W.G., Qin, Z.H., Liu, H.Q., Miao, J.M., Bi, Y.Y., 2008. MODIS-based remote sensing monitoring of grass production in China. Int. J. Remote Sens. 29 (17–18), 5313–5327.
Yang, X., Xu, B., Jin, Y., Li, J., Zhu, X., 2012. On grass yield remote sensing estimation models of China's northern farming-pastoral ecotone. In: Lee, G. (Ed.), Advances in Computational Environment Science. Advances in Intelligent and Soft Computing. Vol. 142. Springer, Berlin, Heidelberg, pp. 281–291.
Yang, S.X., Zhang, W.J., Feng, Q.S., Meng, B.P., Gao, J.L., Liang, T.G., 2016. Monitoring of grassland herbage accumulation by remote sensing using MODIS daily surface reflectance data in the Qingnan Region. Acta Pratacult. Sin. 25 (8), 14–26 (In Chinese).
Yuan, X.L., Li, L.H., Tian, X., Luo, G.P., Chen, X., 2016. Estimation of above-ground biomass using MODIS satellite imagery of multiple land-cover types in China. Remote Sens. Lett. 7 (12), 1141–1149.
Zhang, Y.Y., Zhang, S.F., Zhai, X.Y., Xia, J., 2012. Runoff variation and its response to climate change in the three rivers source region. J. Geogr. Sci. 22 (5), 781–794.
Zhao, F., Xu, B., Yang, X., 2014. Remote sensing estimates of grassland aboveground biomass based on MODIS net primary productivity (NPP): a case study in the Xilingol grassland of northern China. Remote Sens. 6 (6), 5368–5386.
Zhao, H.D., Liu, S.L., Dong, S.K., Su, X.K., Wang, X.X., Wu, X.Y., Wu, L., Zhang, X., 2015. Analysis of vegetation change associated with human disturbance using MODIS data on the rangelands of the Qinghai-Tibet Plateau. Rangel. J. 37, 77–87.